RESEARCH

Subpulse drifting of PSR J1514–4834

Qingying Li[1] · Shijun Dang[1,2,3] · Lunhua Shang[1,3] · Habtamu Menberu Tedila[4] · Xin Xu[1] · Wei Li[1,5,6] · Jie Tian[1] · Yanqing Cai[1] · Zhixiang Yu[1] · Chenbin Wu[1]

Abstract

In this paper, we report the detailed observation of the drift subpulse behavior of PSR J1514–4834 at a central frequency of 1369 MHz using the Parkes 64-m radio telescope. We have found that individual pulses of this pulsar exhibit distinct modulation behaviors for different profile components. The leading and middle components display periodic amplitude modulation with a period of $P_3 = 37.5 \pm 0.8\,P$, and a drifting sub-pulse phenomenon is detected in the phase region of trailing component with the measured drifting periods $P_2 = 7.0 \pm 0.4\,P$ and $P_3 = 37.5 \pm 0.8\,P$. Additionally, it was observed that the leading and trailing components of the pulsar have a clear correlation, the middle and trailing components have a clear anti-correlation, and there is no apparent correlation between the leading and middle components. Moreover, this pulsar deviates from the range of most amplitude-modulated pulsars in the $\dot{E} - P_3$ diagram, but it still falls within the category of subpulse drifting. PSR J1514–4834 exhibits periodic emission modulation and sub-pulse drifting simultaneously in different profile components, which is difficult to understand with the traditional carousel model. Our observational results will provide new observation evidence for theoretical studies of single-pulse emission mechanisms in pulsars.

Keywords Pulsars · Sub-pulse drifting · Periodic modulation (PSR J1514–4834)

1 Introduction

Pulsars are highly rotating neutron stars that serve as a natural laboratory for studying extreme physical conditions, including ultra-high density, temperature, pressure, magnetic fields, and radiation (Lorimer 2005). The pulsar emits periodic signals in strict patterns, resembling a lighthouse, due to the angle formed between its radiation cone and rotation axis, a model referred to as the "lighthouse model" (Gold 1968). When the pulsar's beams intercept the Earth, tele-

Lunhua Shang and Habtamu Menberu Tedila contributed equally to this work.

✉ S. Dang
dangsj@gznu.edu.cn

Q. Li
qyli@gznu.edu.cn

L. Shang
lhshang@gznu.edu.cn

H. Menberu Tedila
habta125@nao.cas.cn

X. Xu
xinxu@gznu.edu.cn

W. Li
weili@gznu.edu.cn

J. Tian
jietian@gznu.edu.cn

Y. Cai
yqcai@gznu.edu.cn

Z. Yu
1257063610@qq.com

C. Wu
1063490546@qq.com

[1] School of Physics and Electronic Science, Guizhou Normal University, Guiyang, 550025, China

[2] Guizhou Radio Astronomical Observatory, Guizhou University, Guiyang, 550001, China

[3] Guizhou Provincial Key Laboratory of Radio Astronomy and Data Processing, Guizhou Normal University, Guiyang, 550025, China

[4] National Astronomical Observatories, Chinese Academy of Sciences, Beijing, 100101, China

[5] Xinjiang Astronomical Observatory, Chinese Academy of Sciences, Urumqi, 830011, China

[6] University of Chinese Academy of Sciences, Beijing, 100049, China

scopes detect a single pulse. These individual pulses appear unstable in shape and phase, but by integration of hundreds of them, a stable pulse profile is obtained. Some pulsars exhibit intriguing phenomena in their single pulses, such as giant pulses, mode changing (Tian et al. 2024), pulse nulling, sub-pulse drifting, and periodic intensity modulation. For instance, the crab pulsar occasionally emits high-intensity nanosecond pulses known as giant pulses (Hankins et al. 2003). Pulsars can switch between multiple radiation states, a phenomenon referred to as mode transformation (Wang et al. 2007), with timescales ranging from seconds to hours. Pulse nulling, associated with the sudden disappearance and resumption of the pulse emission within several periods, has been observed in various pulsars (Rankin 1986; Wang et al. 2007; Ritchings 1976; Vivekanand 1995; Burke-Spolaor et al. 2012; Gajjar et al. 2012). Intermittent pulsar radiation alternates between on and off states, with periods lasting from days to years (Kramer et al. 2006; Camilo et al. 2012; Lorimer et al. 2012; Lyne et al. 2017).

However, one of the pulse-to-pulse variabilities that will create pronounced changes in the shape of a single pulse, is the well-known sub-pulse drifting. The sub-pulse drifting phenomenon was first discovered by Drake and Craft (1968), and often shows that the single pulse will move forward or backward regularly within the ON-pulse window. Since the phenomenon of subpulse drifting was discovered, it has attracted wide attention from researchers. In 1975, Ruderman and Sutherland put forward a theoretical model to explain the phenomenon of sub-pulse drift (Ruderman and Sutherland 1975). They thought that the local area of spark discharge with equal spacing was formed on the emission cone of the pulsar, and the emission cone rotated around the magnetic axis. When the line of sight swept over the local area, we saw the phenomenon of sub-pulse drift, which was called the carousel model (RS). The RS model can only explain the simple and obvious sub-pulse drift phenomenon. It is difficult to explain the complex sub-pulse drift phenomenon, such as drifting mode changing, bi-drifting, the coexistence of drift, and periodic amplitude modulation (Dang et al. 2022; Shang et al. 2022; Basu et al. 2020; Gil and Sendyk 2000; Qiao et al. 2004).

PSR J1514–4834 was first discovered by Noutsos et al. (2008). Basu et al. (2020) reported that this pulsar belongs to the class of pulsars that show periodic modulation drift. However, the previous works only provided basic parameters and did not study the single pulse variation behaviors of this pulsar in detail. In this paper, we carried out the detailed single pulse variation behaviors of PSR J1514–4834, using the two hours of observation data at the central frequency of 1369 MHz with the Parkes 64-m radio telescope. For the first time, we studied the sub-pulse drift of this pulsar in detail. We found that its single pulse variation behaviors are different in different profile components. Our results will provide a new observation sample for the theoretical study of the pulsar radiation mechanism. The observation and data processing process of PSR J1514–4834 is described in Sect. 2, and the results are present in Sect. 3. Section 4 is a brief discussion, and Sect. 5 is the conclusion of the paper.

2 Observations and data processing

The data of PSR J1514–4834 were obtained from the Parkes pulsar data archive[1] and observed by the Parkes 64-m radio telescope. The data were received by the UWL receiver at a center frequency of 1369 MHz and with a bandwidth of 256 MHz. The Parkes Digital Filter Bank Mark-4 (PDFB4) was used to record the data in search mode, with 8-bit sampling, 4 polarizations, 512 channels across the whole band, and a 256 μs sampling interval. The duration of the observation was 2 hours.

We performed basic offline processing of the acquired data. Firstly, we folded and de-dispersed the data using the DSPSR software, incorporating the ephemeris from the ATNF pulsar catalog (PSRCAT-V 5.6) (Manchester et al. 2005). A total of 11,823 single pulses were obtained. Secondly, we removed the radio frequency interference (RFI) using the PAZ and PAZI plugins from the PSRCHIVE pulsar data process software package (Hotan et al. 2004). Finally, we removed the variable baseline and analyzed the subpulse drifting characterize using the PSRSALSA software package (Weltevrede 2016).

3 Results

3.1 The single pulse-stack and average profile

To study the subpulse behavior of PSR J1415–4834, a one-dimensional de-dispersion time series is usually transformed into a two-dimensional array of pulse longitude - pulse series (pulse superposition). This transformation is illustrated in the upper panel of Fig. 1, where 300 consecutive pulses are stacked on the top panel, and the corresponding integrated pulse profile is shown in the bottom panel. From Fig. 1, it can be seen that the integrated pulse profile of this pulsar has multiple peaks, and the trailing component exhibits significant subpulse drifting behavior. To give a detailed investigation of the subpulse drifting in different profile components, we first separated the components of the pulse profile. All of the single pulses are vertically added with the same pulse longitude in continuous pulses to generate a mean pulse profile. Since the flux calibration was

---

[1] https://data.csiro.au/domain/atnf.
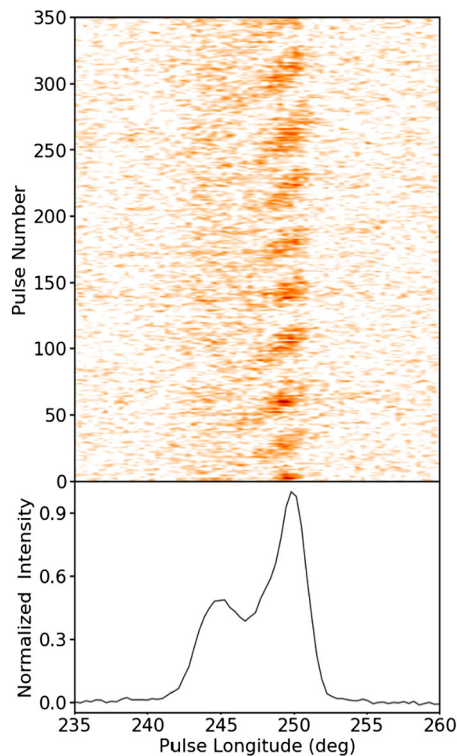
Fig. 1 The single-pulse stack of 300 successive pulses (top panel) and the corresponding normalized mean pulse profile (bottom panel) for PSR J1415–4834

not conducted in this pulsar, we normalized the mean profile. After that, we perform Gaussian fitting on the normalized average pulse profile (Fig. 2). As expected, the average pulse profile of PSR J1514–4834 can be fitted perfectly by three Gaussian components, which means that the mean pulse profile of this pulsar is a three-peak structure. In Fig. 2, the black solid line represents the original mean pulse profile, and the light blue, yellow, and green solid lines represent the Gaussian fitting curves of each component, respectively. The purple solid line is the total Gaussian fitting curve and the vertical red dashed lines are the boundary of each Gaussian component, which divided the mean pulse profile as the leading, middle, and trailing components.

3.2 The single pulse modulation

The drift behavior can be characterized by the pulse amplitude modulation periodicity (P_3, which indicates the repetition time of the sub-pulse along the radiation window of any longitude) and the horizontal separation between adjacent drift bands in pulse longitude (P_2). The P_2 and P_3 usually can be obtained by using the Two-Dimensional Fluctuation Spectrum (2DFS) (Edwards and Stappers 2002; Weltevrede et al. 2006) of the pulse stack. Usually, the existence of subpulses is characterized by measuring the degree of intensity disturbance between different pulses by longitude-resolved

modulation index (Weltevrede et al. 2006). The modulation index, m_i, is defined as follows (Yan et al. 2020):

$$m_i = \frac{\sigma_i}{\mu_i}, \tag{1}$$

where μ_i and σ represent the mean intensity and standard deviation at bin i, respectively. The modulation index serves as a measure of how much the intensity fluctuates from one pulse to the next, thereby indicating the presence of subpulses. In subplot (a) of Fig. 3, the black dots with the error bars represent the m_i of PSR J1514–4834. The leading component has larger m_i than the other two components. However, to determine whether this modulation is chaotic modulation or quasi-periodic modulation, it is necessary to give the 2DFS for further analysis, in which the peak position gives the estimated values of P_3 and P_2. The plots (b), (c), and (d) Fig. 3 show the 2DFS for the leading, middle, and trailing components of PSR J1514–4834, respectively. The side panels stand for the horizontally (left) and vertically (bottom) integrated power. The bottom side panels of (b), (c), and (c) clearly show that the leading and middle components in the pulse window show a peak at $P_2 = 0$, indicating that there is no phase modulation component in these two components. However, the peak value of the trailing component shifts to a direction greater than zero, which indicates that there is a phase modulation component in the trailing component, and its spectral characteristic is $P_2 = 7.0 \pm 0.4\,\mathrm{P}$. For the left side panels of (b), (c), and (c), it is clear that the peak values of the three components shift to a positive direction in the pulse window, which indicates that all three components have amplitude modulation components, and their spectral characteristics are $P_3 = 37.5 \pm 0.8\,\mathrm{P}$. For a certain pulsar, if both P_2 and P_3 have nonzero values, it indicates that the pulsar has subpulse drifting. If only P_3 is nonzero and P_2 is equal to zero, it indicates that the pulsar has periodic amplitude modulation. Otherwise, it is an unidentifiable single pulse variation. Hence, for PSR J1514–4834, the 2DFS results indicate that its leading and middle components have quasi-periodic amplitude modulation, and the trailing component has subpulse drifting.

3.3 The correlation between the pulse profile components

The above Sect. 3.1 seems to indicate that there is a certain phase connection between the emission behavior of the leading, middle, and trailing components. To further confirm this, we have obtained the longitude-longitude correlation among these three components in Fig. 4 with zero delay. The left and top side windows show the normalized average pulse profile. The main panel shows the correla-

Fig. 2 The black solid line is the mean pulse profile of PSR J1514–4834. The light blue, yellow, and green solid lines represent the components of the Gaussian fitting curve of the mean pulse profile, respectively. The purple solid line is the total Gaussian fitting curve and two vertical red dashed lines are the boundary of each Gaussian component. The bottom panel is the residual of Gaussian fitting
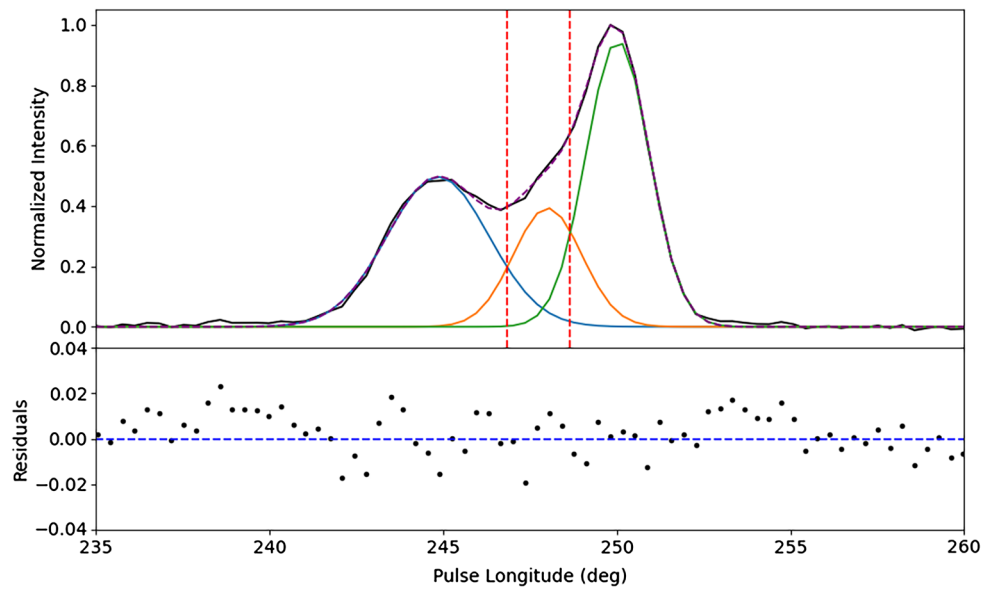

Fig. 3 Fluctuation analysis for PSR J1514–4834. The upper panel contains multiple subplots: (a) illustrates the averaged pulse profile and the modulation indices of pulse-to-pulse perturbation variations. (b), (c), and (d) display the two-dimensional Fourier analyses (2DFS) for the leading, middle, and trailing components, respectively
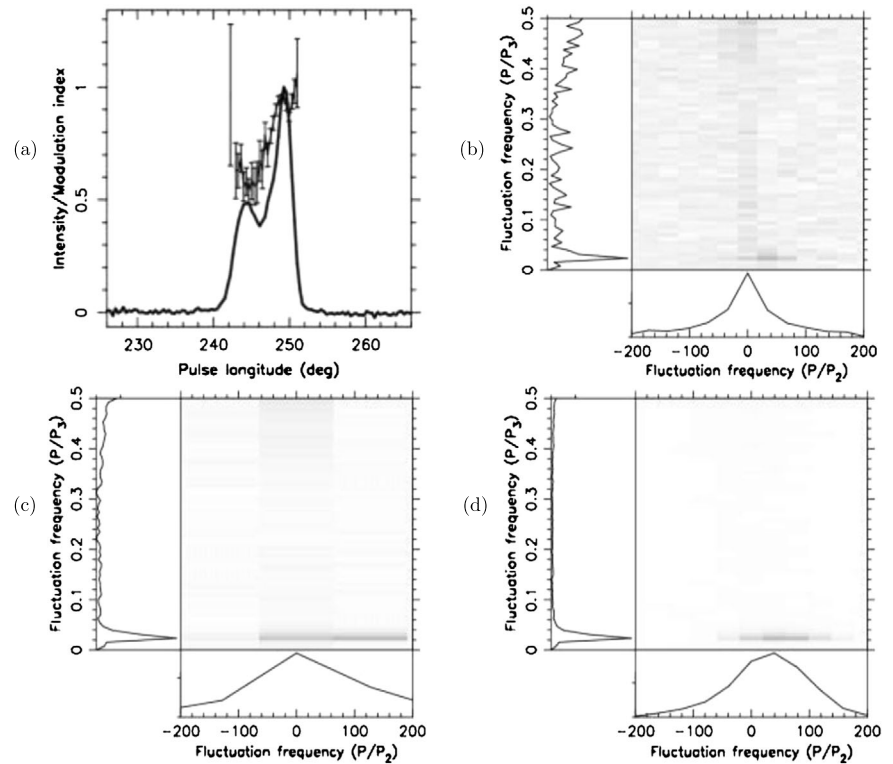
tion between these three components, and the red diagonal line shows the auto-correlation results of the components. The vertical and horizon green dotted lines are the boundary lines between the three components. The color in the main panel from blue to red indicates the result of the correlation from negative to positive. Figure 4 clearly shows a negative correlation between the middle and trailing components, but there is no obvious correlation between the middle and leading components. The leading and trailing components have

a strong correlation. This means that the emission of the leading component is inversely correlated with the middle component but positively correlated with the leading component. All three components have a modulation period of $37.5 \pm 0.8\,\mathrm{P}$, indicating a 37.5 P delay between the middle component and the trailing component, similar to the so-called phase-locking phenomenon (Kou et al. 2021). The correlation between different profile components indicates that the physical mechanisms are related or opposite.
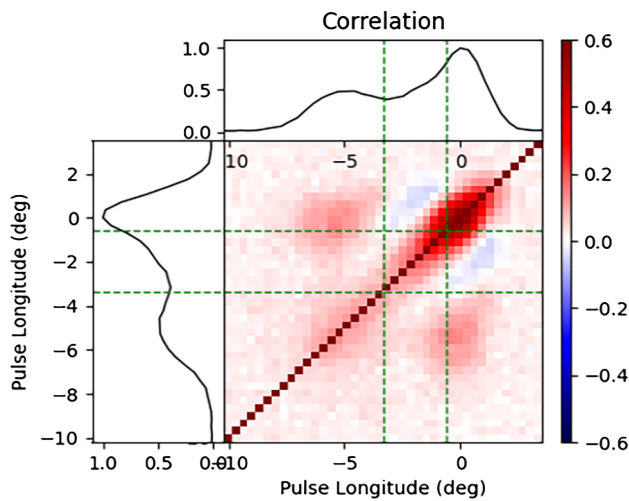
Fig. 4 The longitude-longitude correlation among leading, middle, and trailing components with zero delay. The left and bottom windows show the normalized mean pulse profile. the green dashed lines are the dividing lines of the three components

3.4 Pulse energy distribution

The phenomenon of pulse nulling has been observed in many pulsars, in which the pulse emission suddenly or gradually turns off in several pulse periods and then suddenly or gradually turns on (Ritchings 1976; Rankin 1986; Biggs 1992; Vivekanand 1995; Wang et al. 2007; Burke-Spolaor et al. 2012; Gajjar et al. 2012). The time scale of nulling varies from seconds to hours. To verify whether PSR J1514–4834 has potential nulling behavior, we statistically analyze the energy of a single pulse.

The traditional method used to measure the nulling fraction (NF) is given by Ritchings (1976). In this method, the threshold used to split the nulling and burst pulse is defined by noise, and the accuracy depends on the sensitivity of the telescope. In particular, the on-pulse histogram of pulsars with low signal-to-noise (S/N) ratio will approach the off-pulse histogram, which will lead to an overestimate of NF, such as Kaplan et al. (2018) and Anumarlapudi et al. (2023). For PSR J1514–4834, the S/N is low, so we adopt a more robust mixed model Anumarlapudi et al. (2023) to verify whether the emissions have a nulling pulse. Similar to the method of Ritchings (1976), this method relies on the histogram, but it employs the Markov chain Monte Carlo (MCMC) to fit n Gaussian distributions to the on-pulse region to form null and non-nulling distributions (Anumarlapudi et al. 2023). Then, In the budgetary estimate, Gaussian fitting in the nulling region is compared with Gaussian fitting in the off-pulse region, to estimate NF and get its uncertainty, which the Ritchings method is not easy to provide.

This method is realized by the published software textscpulsar_nulling.[2]

To obtain the energy distribution histogram, we select the region with an integration pulse profile energy higher than 3 times the standard deviation (3σ) as the on-pulse window, and the others as the off-pulse window. The left figure of Fig. 5 shows the energy distribution histogram of PSR J1514–4834, we find that the on-pulse histogram is close to the off-pulse histogram, which makes the pulses with energy less than zero appear obviously in the on-pulse histogram. The off-pulse histogram is fit with a simple Gaussian (black solid line), whereas the on-pulse histogram is fit with a combination of multi-component Gaussian (red solid line). The multi-component Gaussian is composed of a Gaussian component that represents real emission (grey dot-dashed line), and a nulling Gaussian component (blue dot-dashed line) that is a scaled version of the off-pulse Gaussian. Due to the very small NF of this pulsar, which is almost zero, the red solid line and the gray dashed line are almost overlapping, making it difficult to distinguish them at the resolution of this figure. The right figure of Fig. 5 shows the corner plots for 2-component Gaussian fit to the ON-OFF histograms parameterized by the means [μ_0, μ_1], standard deviations [σ_0, σ_1], and the nulling fraction NF. The value of NF is $0.001^{+0.002}_{-0.001}$, this value is very small and can be regarded as 0. We guess that the reason for this phenomenon may be the existence of weak pulses in PSR J1514–4834 or Gaussian random noise caused by telescope noise. To further confirm this speculation, we extracted 958 pulses with pulse energy less than zero in the on-pulse window and obtained the corresponding normalization integration pulse profile(as shown in Fig. 6). We can see a clear pulse profile with an S/N ratio of 9, which further confirms that PSR J1514–4834 has no nulling.

4 Discussions

Various theoretical models explaining the drift subpulses have been proposed shortly after their discovery. Currently, the most comprehensive theoretical model is the well-known carousel model proposed by Ruderman and Sutherland (1975). Ruderman proposed that the binding energy of ions on the surface of neutron stars is as high as 14kev under a strong magnetic field (Ruderman and Sutherland 1975). Because of the large ion binding energy on the surface of the neutron star, positively charged particles can't leave the neutron star freely, so in the magnetosphere near the surface of the neutron star in the polar cap region, a region where the charge is evacuated will be formed, which is called gap. There will be a strong electric field in it, which is parallel to the magnetic field. γ photons from the background

---

[2]https://github.com/AkashA98/pulsar_nulling.
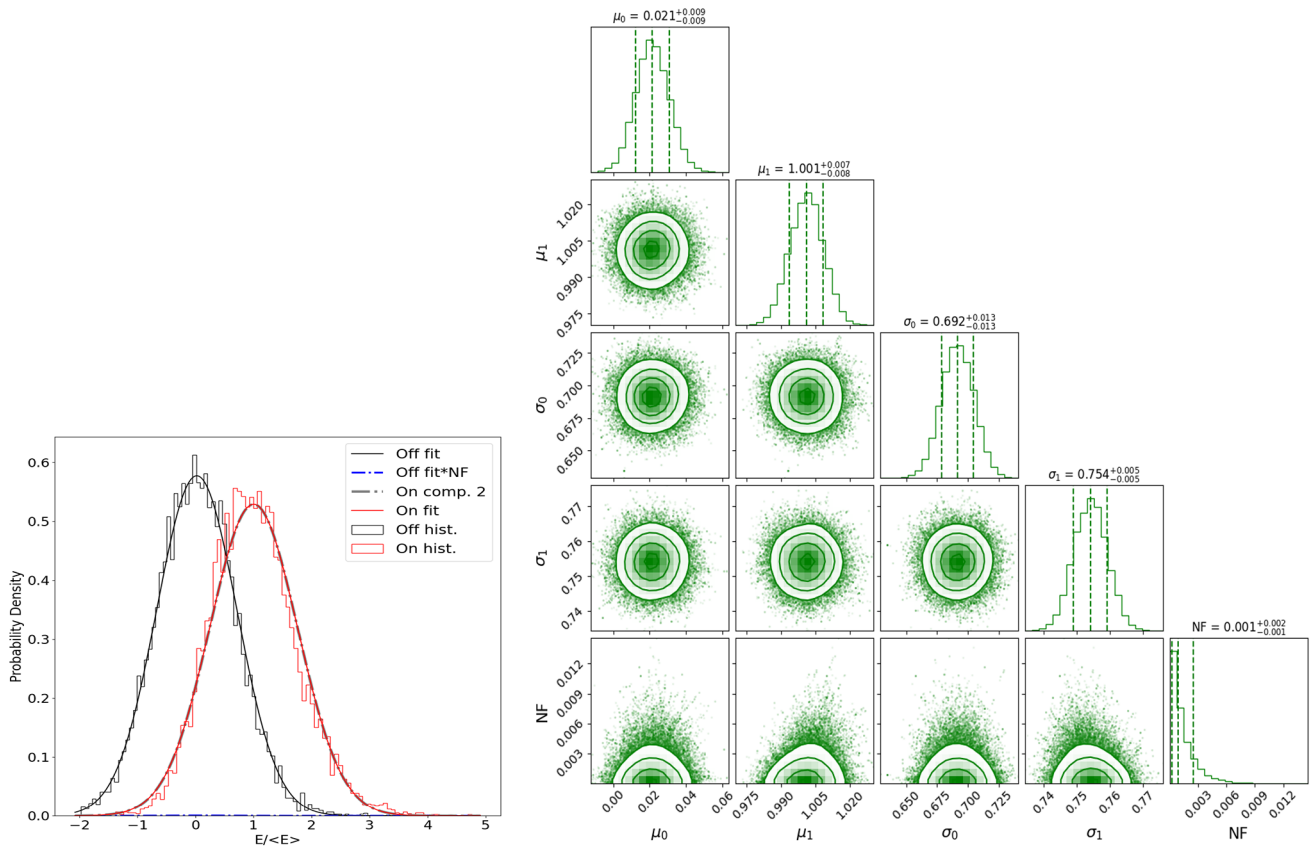
Fig. 5 Left: two-component Gaussian model fits for the ON and OFF histograms of PSR J1514-4834(in red and black, respectively). The off-pulse histogram is fit with a simple Gaussian (black solid line), whereas the on-pulse histogram is fit with a multicomponent Gaussian (red solid line). The multicomponent Gaussian is composed of a Gaussian that represents real emission (grey dot-dashed line), and a nulling Gaussian (blue dot-dashed line) that is a scaled version of the off-pulse Gaussian. Right: corner plots for 2-component Gaussian fit to the ON-OFF histograms parameterized by the means $[\mu_0, \mu_1]$, standard deviations $[\sigma_0, \sigma_1]$, and the nulling fraction NF

Fig. 6 The normalized pulse profile of 958 pulses with the pulse energy of the ON-pulse window less than zero
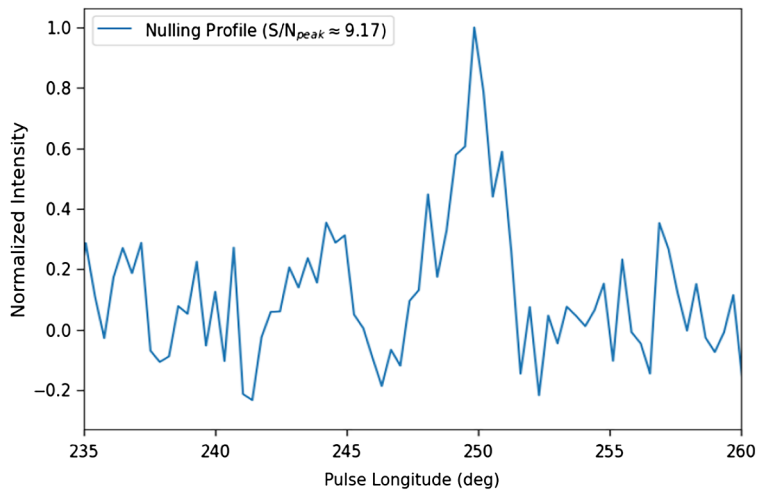
of the Milky Way galaxy enter the vacuum gap, producing positive and negative electron pairs. Positive and negative electrons are accelerated in the electric field to become high-energy electrons, thus generating γ photons, which in turn generate electron pairs, and so on, forming a cascade avalanche process until the gap is "broken down" (Ruderman and Sutherland 1975). The secondary particles leaving the gap produce radio emissions. The carousel model proposes that $E \times B \neq 0$ in the inner gap, and the radiation area rotates around the magnetic axis like a "Carousel", and

Fig. 7 Pulsar period modulation (PM) in relation to spin-slowing energy loss ($\dot{E}$)
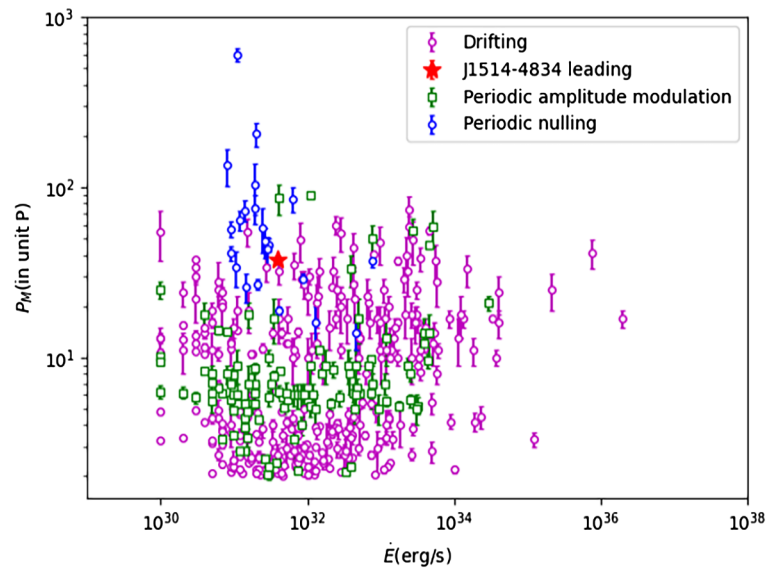
the sub-pulse will move forward or backward regularly in the radiation window, thus forming the phenomenon of sub-pulse drifting. The carousel model proposed that the radiation cone is hollow, so the central radiation beam cannot be obtained. However, the carousel model can only be used to explain single, regular sub-pulse drifting phenomena, but cannot explain "Bi-drifting" and drift mode switch. For PSR J1514–4834, its leading and middle components have amplitude modulation and the trailing component has sub-pulse drifting, which will challenge the carousel model.

A large sample study of pulsars with subpulse drifts reveals two important characteristics of subpulse drifts: the relationship between the drift period (P_3) and the energy loss rate ($\dot{E}$) is negatively correlated; the drift pattern evolves with the geometry of the line-of-sight (LOS), and the drift of each component in the pulse sequence is different. (Rankin 1986; Gil and Sendyk 2000; Deshpande and Rankin 2001; Weltevrede et al. 2006, 2007; Basu et al. 2016; Basu and Mitra 2018; Basu et al. 2019, 2020; Song et al. 2023). Basu et al. (2019) found that P_3 is inversely correlated with $\dot{E}$, and low $\dot{E}$ typically with a larger P_3 value. Especially, pulsars with a cone component typically with $\dot{E} < 5 \times 10^{32}\ \mathrm{erg\,s^{-1}}$, are more likely to have drifting subpulses (see also Rankin (1986)). Pulsars with $\dot{E} > 5 \times 10^{32}\ \mathrm{erg\,s^{-1}}$ have a core-dominated pulse profile and amplitude modulation (no detectable drift), with a larger P_3 value. To further discuss the radiative properties of the pulsar PSR J1514–4834, we give the $\dot{E} - P_3$ relationship diagram in Fig. 7 utilized data of 474 pulsars from Basu et al. (2020) and Song et al. (2023). The magenta square error bar corresponds to drift, the red star error bar corresponds to PSR J1514–4834, the green square error bar corresponds to periodic amplitude modulation, the black square error bar corresponds to periodic modulation, and the blue square error bar corresponds to peri-

odic nulling. Periodically modulated pulsars are widely distributed in $\dot{E} - P_3$ diagram and their amplitude modulation does not depend on $\dot{E}$. Song et al. (2023) further explained that the relationship between P_3 and $\dot{E}$ was weaker, and showed that the correlation ratio was stronger in the combination of P and $\dot{P}$ values closer to the death line. Basu et al. (2020) also show that the sub-pulse drift is different from other periodic modulations, but there are overlapping behaviors among the three groups of periodic modulations. PSR J1514–4834 is a pulsar with higher $\dot{E} = 3.9 \times 10^{32}\ \mathrm{erg\,s^{-1}}$ and $P_3 = 37.5 \pm 0.8\ \mathrm{P}$. Although it deviates from the range of most amplitude-modulated pulsars, it still falls within the category of subpulse drifting. Moreover, subpulse drifting varies greatly between different profile types. Classification of pulse profile types can help us understand the evolutionary relationship between the drift pattern and the geometry of the LOS.

When LOS passes through the periphery of the radiation beam, it will show an obvious drift band and large phase ($>100°$) change and organized coherent phase modulation sub-pulse drift, which is usually related to the pulse profile types of conal single (S_d) and conal double (D) (Basu et al. 2019). When the LOS passes through more internal radiation beams, the sub-pulse drift behavior will be more complicated. The slope of the phase will be reversed, and the switching phase modulation sub-pulse with sudden 180° jump of adjacent components will drift, which usually corresponds to two pulse profile types: conal triple ($_cT$) and conal quadruple ($_cQ$) (Basu et al. 2019). When the LOS passes through the center of the radiation beam, the core component has no drift, and it is observed that the significant drift behavior of the cone component usually has a low phase change (Basu et al. 2019). For PSR J1514–4834, its leading and middle components have no phase modulation, only

significant amplitude modulation, but its trailing component has phase modulation, and the phase change ($<100°$) is shallower than the coherent phase drift. The drift characteristics of each component of PSR J1514–4834 are similar to low-mixed phase modulation, which usually corresponds to two pulse profile types: T and M (Basu et al. 2019). Furthermore, from Fig. 4, we can see that there are important dynamic connections between the various components of this pulsar. Firstly, the three components share a $37.5 \pm 0.8\,P$ intensity modulation period. Secondly, the leading and trailing components have a strong positive correlation, while the intermediate component has a strong negative correlation with the trailing component and no significant correlation with the leading component. According to previous theories, subpulse drift usually occurs in the cone component, while intensity modulation can occur in both the cone and core components, indicating that the leading and trailing components may be cone components, while the middle component is a core component. Rankin (Rankin 1986) proposed that the sub-pulse drifting is mainly a cone phenomenon, while the low-frequency periodic modulation seen in the core component belongs to different physical phenomena. Therefore, we look forward to using more sensitive radio telescopes (such as the SKA) in the future to conduct polarization observations of PSR J1514–4834. It would be interesting to investigate whether the leading and trailing components of this pulsar are indeed cone components and whether the intermediate component is a core component. This could provide valuable insights into the physical mechanisms behind the unique subpulse behavior of this pulsar.

5 Summary

In this paper, we investigated the single pulse emission properties of PSR J1514–4834 based on two hours of observations with the Parkes 64-m radio telescope at 1369 MHz for the first time. Our main results are as follows:

1. We employed the 2DFS technique to obtain the subpulse variation behavior of the leading, middle, and trailing components of PSR J1514–4834. The leading and middle components display amplitude-modulated, while the trailing component exhibits subpulse drifting. The three components share an intensity modulation period, $P_3 = 37.5 \pm 0.8\,P$, and the trailing component has a separation period, $P_2 = 7 \pm 0.4\,P$.
2. Using the longitude-longitude correlation among these three components, we found that the intensity of the leading component is strongly correlated with the trailing component, but strongly inverse correlated with the middle component. There is no obvious correlation detected between the leading and the middle components.

The correlation between different profile components indicates that the physical mechanisms are related or opposite.

The unique subpulse variation behaviors of PSR J1514–4834 will provide new observation evidence for theoretical studies of single-pulse emission mechanisms in pulsars. Unfortunately, due to the lack of polarization observation data, we cannot provide a more detailed analysis of its radiation variation behavior. We expect to use more sensitive radio telescopes, such as SKA, to conduct polarization observations of PSR J1514–4834 in the future. This is crucial for studying the physical mechanisms underlying its single pulse variation behavior.

Declarations

References

Anumarlapudi, A., Swiggum, J.K., Kaplan, D.L., et al.: A pilot study of nulling in 22 pulsars using mixture modeling. Astrophys. J. **948**(1), 32 (2023). https://doi.org/10.3847/1538-4357/acbb68. arXiv:2301.13258 [astro-ph.HE]

Basu, R., Mitra, D.: Characterizing the nature of subpulse drifting in pulsars. Mon. Not. R. Astron. Soc. **475**(4), 5098–5107 (2018). https://doi.org/10.1093/mnras/sty178. arXiv:1801.06038 [astro-ph.HE]

Basu, R., Mitra, D., Melikidze, G.I., et al.: Meterwavelength Single-Pulse Polarimetric Emission Survey. II. The phenomenon of drifting subpulses. Astrophys. J. **833**(1), 29 (2016). https://doi.org/10.3847/1538-4357/833/1/29. arXiv:1608.00050 [astro-ph.HE]

Basu, R., Mitra, D., Melikidze, G.I., et al.: Classification of subpulse drifting in pulsars. Mon. Not. R. Astron. Soc. **482**(3), 3757–3788 (2019). https://doi.org/10.1093/mnras/sty2846. arXiv:1810.08423 [astro-ph.HE]

Basu, R., Mitra, D., Melikidze, G.I.: Periodic modulation: newly emergent emission behavior in pulsars. Astrophys. J. **889**(2), 133 (2020). https://doi.org/10.3847/1538-4357/ab63c9. arXiv:1912.06868 [astro-ph.HE]

Biggs, J.D.: An analysis of radio pulsar nulling statistics. Astrophys. J. **394**, 574 (1992). https://doi.org/10.1086/171608

Burke-Spolaor, S., Johnston, S., Bailes, M., et al.: The High Time Resolution Universe Pulsar Survey - V. Single-pulse energetics and modulation properties of 315 pulsars. Mon. Not. R. Astron. Soc. **423**(2), 1351–1367 (2012). https://doi.org/10.1111/j.1365-2966.2012.20998.x. arXiv:1203.6068 [astro-ph.SR]

Camilo, F., Ransom, S.M., Chatterjee, S., et al.: PSR J1841-0500: a radio pulsar that mostly is not there. Astrophys. J. **746**(1), 63 (2012). https://doi.org/10.1088/0004-637X/746/1/63. arXiv:1111.5870 [astro-ph.GA]

Dang, S.J., Shang, L.H., Lin, L., et al.: Subpulse drifting of PSR J1110-5637. Res. Astron. Astrophys. **22**(6), 065011 (2022). https://doi.org/10.1088/1674-4527/ac6aab

Deshpande, A.A., Rankin, J.M.: The topology and polarization of sub-beams associated with the 'drifting' sub-pulse emission of pulsar B0943+10 - I. Analysis of Arecibo 430- and 111-MHz observations. Mon. Not. R. Astron. Soc. **322**(3), 438–460 (2001). https://doi.org/10.1046/j.1365-8711.2001.04079.x. arXiv:astro-ph/0010048 [astro-ph]

Drake, F.D., Craft, H.D.: Second periodic pulsation in pulsars. Nature **220**(5164), 231–235 (1968). https://doi.org/10.1038/220231a0

Edwards, R.T., Stappers, B.W.: Drifting sub-pulse analysis using the two-dimensional Fourier transform. Astron. Astrophys. **393**, 733–748 (2002). https://doi.org/10.1051/0004-6361:20021067. arXiv:astro-ph/0207472 [astro-ph]

Gajjar, V., Joshi, B.C., Kramer, M.: A survey of nulling pulsars using the giant meterwave radio telescope. Mon. Not. R. Astron. Soc. **424**(2), 1197–1205 (2012). https://doi.org/10.1111/j.1365-2966.2012.21296.x. arXiv:1205.2550 [astro-ph.SR]

Gil, J.A., Sendyk, M.: Spark model for pulsar radiation modulation patterns. Astrophys. J. **541**(1), 351–366 (2000). https://doi.org/10.1086/309394. arXiv:astro-ph/0002450 [astro-ph]

Gold, T.: Rotating neutron stars as the origin of the pulsating radio sources. Nature **218**(5143), 731–732 (1968). https://doi.org/10.1038/218731a0

Hankins, T.H., Kern, J.S., Weatherall, J.C., et al.: Nanosecond radio bursts from strong plasma turbulence in the Crab pulsar. Nature **422**(6928), 141–143 (2003). https://doi.org/10.1038/nature01477

Hotan, A.W., vanStraten, W., Manchester, R.N.: PSRCHIVE and PSRFITS: an open approach to radio pulsar data storage and analysis. Publ. Astron. Soc. Aust. **21**(3), 302–309 (2004). https://doi.org/10.1071/AS04022. arXiv:astro-ph/0404549 [astro-ph]

Kaplan, D.L., Swiggum, J.K., Fichtenbauer, T.D.J., et al.: A Gaussian mixture model for nulling pulsars. Astrophys. J. **855**(1), 14 (2018). https://doi.org/10.3847/1538-4357/aaab62. arXiv:1801.09598 [astro-ph.IM]

Kou, F.F., Yan, W.M., Peng, B., et al.: Periodic and phase-locked modulation in PSR B1929+10 observed with FAST. Astrophys. J. **909**(2), 170 (2021). https://doi.org/10.3847/1538-4357/abd545. arXiv:2012.10156 [astro-ph.HE]

Kramer, M., Lyne, A.G., O'Brien, J.T., et al.: A periodically active pulsar giving insight into magnetospheric physics. Science **312**(5773), 549–551 (2006). https://doi.org/10.1126/science.1124060. arXiv:astro-ph/0604605 [astro-ph]

Lorimer, D.R.: Binary and millisecond pulsars. Living Rev. Relativ. **8**(1), 7 (2005). https://doi.org/10.12942/lrr-2005-7. arXiv:astro-ph/0511258 [astro-ph]

Lorimer, D.R., Lyne, A.G., McLaughlin, M.A., et al.: Radio and X-ray observations of the intermittent pulsar J1832+0029. Astrophys. J. **758**(2), 141 (2012). https://doi.org/10.1088/0004-637X/758/2/141. arXiv:1208.6576 [astro-ph.HE]

Lyne, A.G., Stappers, B.W., Freire, P.C.C., et al.: Two long-term intermittent pulsars discovered in the PALFA survey. Astrophys. J. **834**(1), 72 (2017). https://doi.org/10.3847/1538-4357/834/1/72. arXiv:1608.09008 [astro-ph.HE]

Manchester, R.N., Hobbs, G.B., Teoh, A., et al.: The Australia telescope national facility pulsar catalogue. Astron. J. **129**(4), 1993–2006 (2005). https://doi.org/10.1086/428488. arXiv:astro-ph/0412641 [astro-ph]

Noutsos, A., Johnston, S., Kramer, M., et al.: New pulsar rotation measures and the galactic magnetic field. Mon. Not. R. Astron. Soc. **386**(4), 1881–1896 (2008). https://doi.org/10.1111/j.1365-2966.2008.13188.x. arXiv:0803.0677 [astro-ph]

Qiao, G.J., Lee, K.J., Zhang, B., et al.: A model for the challenging "bi-drifting" phenomenon in PSR J0815+09. Astrophys. J. Lett. **616**(2), L127–L130 (2004). https://doi.org/10.1086/426862. arXiv:astro-ph/0410479 [astro-ph]

Rankin, J.M.: Toward an empirical theory of pulsar emission. III. Mode changing, drifting subpulses, and pulse nulling. Astrophys. J. **301**, 901 (1986). https://doi.org/10.1086/163955

Ritchings, R.T.: Pulsar single pulse intensity measurements and pulse nulling. Mon. Not. R. Astron. Soc. **176**, 249–263 (1976). https://doi.org/10.1093/mnras/176.2.249

Ruderman, M.A., Sutherland, P.G.: Theory of pulsars: polar gaps, sparks, and coherent microwave radiation. Astrophys. J. **196**, 51–72 (1975). https://doi.org/10.1086/153393

Shang, L.H., Bai, J.T., Dang, S.J., et al.: The "bi-drifting" subpulses of PSR J0815+0939 observed with the Five-hundred-meter Aperture Spherical Radio Telescope. Res. Astron. Astrophys. **22**(2), 025018 (2022). https://doi.org/10.1088/1674-4527/ac424d

Song, X., Weltevrede, P., Szary, A., et al.: The thousand-pulsar-array programme on MeerKAT - VIII. The subpulse modulation of 1198 pulsars. Mon. Not. R. Astron. Soc. **520**(3), 4562–4581 (2023). https://doi.org/10.1093/mnras/stad135. arXiv:2301.04067 [astro-ph.HE]

Tian, J., Xu, X., Bai, J., et al.: Investigation of states switch properties of PSR J1946+1805 with the FAST. Astrophys. Space Sci. **369**(2), 21 (2024). https://doi.org/10.1007/s10509-024-04284-9

Vivekanand, M.: Observation of nulling in radio pulsars with the Ooty Radio Telescope. Mon. Not. R. Astron. Soc. **274**(3), 785–792 (1995). https://doi.org/10.1093/mnras/274.3.785

Wang, N., Manchester, R.N., Johnston, S.: Pulsar nulling and mode changing. Mon. Not. R. Astron. Soc. **377**(3), 1383–1392 (2007). https://doi.org/10.1111/j.1365-2966.2007.11703.x. arXiv:astro-ph/0703241 [astro-ph]

Weltevrede, P.: Investigation of the bi-drifting subpulses of radio pulsar B1839-04 utilising the open-source data-analysis project PSRSALSA. Astron. Astrophys. **590**, A109 (2016). https://doi.org/10.1051/0004-6361/201527950. arXiv:1605.06413 [astro-ph.HE]

Weltevrede, P., Edwards, R.T., Stappers, B.W.: The subpulse modulation properties of pulsars at 21 cm. Astron. Astrophys. **445**(1), 243–272 (2006). https://doi.org/10.1051/0004-6361:20053088. arXiv:astro-ph/0507282 [astro-ph]

Weltevrede, P., Stappers, B.W., Edwards, R.T.: The subpulse modulation properties of pulsars at 92 cm and the frequency dependence of subpulse modulation. Astron. Astrophys. **469**(2), 607–631 (2007). https://doi.org/10.1051/0004-6361:20066855. arXiv:0704.3572 [astro-ph]

Yan, W.M., Manchester, R.N., Wang, N., et al.: Periodic mode changing in PSR J1048-5832. Mon. Not. R. Astron. Soc. **491**(4),

4634–4641 (2020). https://doi.org/10.1093/mnras/stz3399. arXiv: 1912.01165 [astro-ph.HE]

Publisher's Note Springer Nature remains neutral with regard to jurisdictional claims in published maps and institutional affiliations.